NANOINDENTATION AND MICROSTRUCTURE ANALYSIS OF HIGH CHROMIUM WHITE CAST IRON FOR MACHINABILITY STUDY

L. Chen[1], S. Iyengar[2], J. M. Zhou[1], K. Turba[2], J. E. Ståhl[1]

[1] *Division of Production and Materials Engineering, Lund University, Box 118, Lund, Sweden*
[2] *Division of Materials Engineering, Lund University, Box 118, Lund, Sweden*

ling.chen@iprod.lth.se

Abstract: The investigation carried out in this paper analyses the microstructure of the HCCI materials before and after the heat treatment using nanoindentation technique and scanning electron-microscopy in order to understand the effect of metallurgical factors such as morphology and volume fraction of carbides as well as mechanical properties on the further study of machinability of the materials. Present results show that changes in carbon and silicon contents as well as heat treatment strongly affect the mechanical properties and their variation in the material. The sample with higher C-Si contents has more eutectic carbides in a bainite matrix leading to a lower hardness in the as cast sample, while the sample with lower C-Si contents has higher hardness with austenite and martensite in the matrix. After annealing treatment, both sets of materials are softer than before, with the higher C-Si material being a little harder due to the presence of more eutectic carbides. Both low and high C-Si samples show similar hardness after the hardening treatment and the microstructure consists of secondary carbides and martensite surrounding the interconnecting eutectic carbides. In general, the larger volume fraction of the primary carbides associated with higher C-Si contents leads to a decrease in hardness.

Keywords: machinability, white cast iron, microstructure, nanoindentation, heat treatment

1. INTRODUCTION

It is well known that machinability of a material is strongly related to its microstructure and mechanical properties. Factors such as grain size, phases present and their relative amounts and mechanical properties such as hardness play an important role and determine the extent of tool wear, stability and surface quality during machining (Tabrett, 1997). In general, High chromium white cast irons (HCCI) offer exceptional abrasion and corrosion resistance due to the substantial presence of chromium rich carbides and are used extensively in applications where superior wear resistance is desired (Fernandez-Pariente and Belzunce, 2008). The abrasion resistance of these materials is profoundly influenced by the microstructure and the micro mechanical properties of the material (Turenne, et al., 1989). These materials are generally associated with poor machinability due to the presence of large amounts of hard eutectic carbides distributed unevenly in the matrix (Tsypin, 1969), which can damage the cutting tool rapidly (Huang, et al., 2006). The performance of HCCI materials can be improved by heat treatment (Karantzalis, et al., 2009) and composition changes (Kosasu, et al., 2012). Often, the materials are readily cast into parts needed in machinery for forming, crushing and grinding as well as other durable parts in the tooling industry affected by abrasive wear. In this study, an attempt has been made to understand the effect of metallurgical factors such as morphology and volume fraction of carbides as well as mechanical properties on the machinability of the materials. The microstructures of HCCI materials with different compositions (carbon

and silicon contents) have been characterized in the as-cast as well as annealed and hardened conditions using scanning electron microscopy, energy dispersive spectroscopy and nanoindentation techniques.

2. MATERIAL PREPARATION AND TEST SETUP

High chromium white cast iron is virtually a composite material with a metallic matrix reinforced with carbide particles. The composition of the matrix phase can be suitably modified to achieve a proper balance between resistance to abrasion and the toughness needed to withstand repeated impact (Karantzalis, et al., 2009).
In this study, two groups of high chromium cast irons were prepared, with a maximum chromium content of 25.7 *wt.*%. The alloys were cast into rounds (66 *mm* in diameter) and cut into pieces of 10x10x5 mm^3 using a wire electrical discharge machine.

The groups were divided on the basis of carbon-silicon (C-Si) contents. The group with lower C-Si content had 2.71 *wt.*% C and 0.8 *wt.*% Si and the group with higher C-Si content had 2.95 *wt.*% C and 1.47 *wt.*% Si. A total of six samples were prepared. Of the three samples per group, one corresponded to the as cast condition, the other two to the annealed (heating to 930 °C, holding time:1.5h, cooling to 650 °C, holding time: 1h, cooling to 600 °C, holding time 2 h, cooled to room temperature) and the hardened conditions (heating to 940 °C, holding time 2h, quenched to room temperature).

All the specimens were mounted, ground, and polished following standard metallographic procedure. The final polishing procedure was done SiO_2 particles (0.04 μm). The etchant in the test is modified glyceregia (Vander Voort, 2004). All the nanoindentations were made in compliance with ISO 14577 and ASTM E2546-07. Metallographic examination was conducted using an enironmental scanning electronic microscope (ESEM, Philips XL-30). The micromechanical properties were tested on a nanoindentation instrument using the NanoTest Vantage system with a loading range of 0.01 to 500 *mN* and a Berkovich diamond indenter with a tip radius of 120 *nm*. In the present work, the applied load was chosen to be 5 *mN* in order to minimize the influence of grain size and nanohardness was measured at 400 grid points over a randomly selected area of 400 μm × 400 μm. All the indentations in the tests were load controlled and the maximum load is the same for all the measurements.

3. METALLOGRAPHIC EXAMINATION USING SEM

Samples with different compositions show differences in microstructures. The as cast sample with the lower C-Si content (Cr/C ratio~9.34), exhibited typical hypoeutectic microstructure in which the matrix contains the primary austenite dendrites with needle-like martensite (Asensio, et al., 2003). The martensite surrounds the interconnecting network of brittle, faceted M_7C_3 eutectic carbides. In contrast, the as cast sample with the higher C-Si content (Cr/C ratio~8.71) has a hypereutectic microstructure in which the austenite is mainly transformed to bainite in the matrix and the primary eutectic carbides are distributed in some regions which are surrounded by discontinious eutectic carbides. Through the annealing procedure, the austenite is transformed to bainite in the sample with lower C-Si content and to pearlite in the sample with higher C-Si content. Plenty of secondary carbide particles are observed within the matrix in both samples. The presence of martensite in the matrix was observed in both the samples after the hardening treatment. However, it also led to the formation of very fine-sized secondary carbide particles in the matrix. In all the samples, regardless of the initial composition, no significant change in the morphology of the eutectic carbide was observed after heat treatment. The following sections describe the influence of heat treatment on the microstructures and phase evolution in the samples in greater detail.

3.1. Microstructural analysis of samples with lower C-Si contents

Materials with lower C-Si contents were studied in three different conditions: as cast, annealed and hardened. In general, the solidification of lower C-Si white cast iron commences with the formation of austenite dendrites.
As the remaining liquid freezes, a mixture of M_7C_3 and austenite is formed. During the solidification process, the formation of eutectic carbides involves the redistribution of carbon and other alloying elements present in the austenite, there is some depletion of alloying elements over a narrow zone at the carbide-austenite interface. The lack of carbon and alloying elements in this zone increases the martensite starting (M_s) temperature, which leads to the transformation of austenite to martensite during the subquent cooling cycle(Hinckley, et al., 2008). Observations show that the eutectic carbides are not affected significantly by the annealing or hardening heat

treatments. While the matrix transforms mainly to bainite with secondary carbides after annealing, a martensite matrix with secondary carbides is formed after the hardening treatment. It is important to note that no secondary carbide was observed in the as cast sample and it can be presumed that they were dissolved in the austenite matrix (Asensio, et al., 2003). As expected, secondary carbides in the hardened sample are finer than in the annealed sample (Fig. 1).

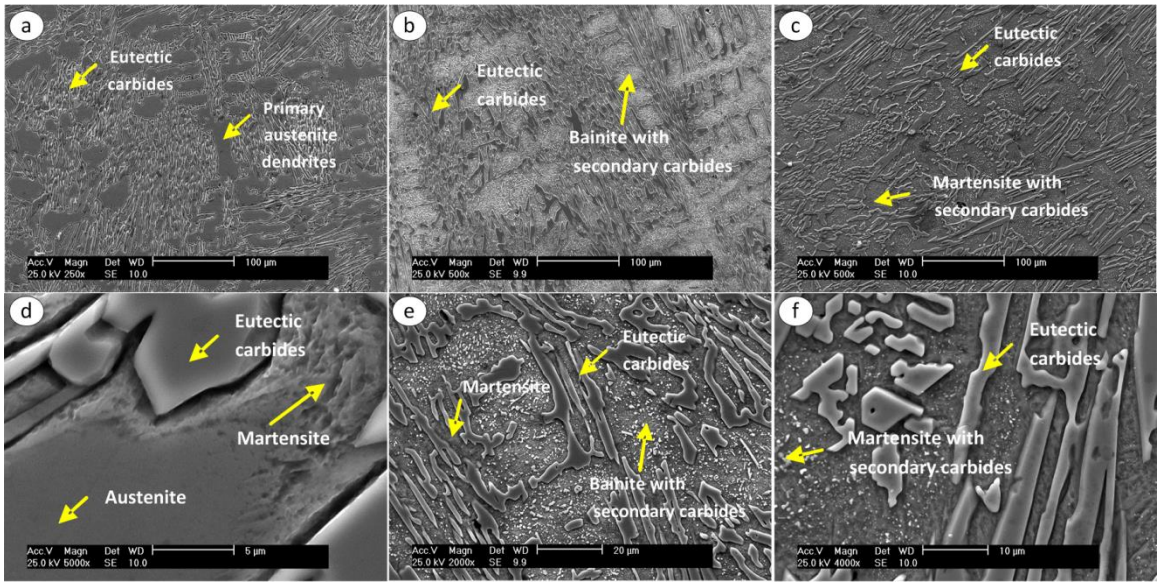

Fig. 1. Microstructures of high chromium white cast irons (lower C-Si contents) in the as cast (a, d), annealed (b,e) and hardened condition (c, f).

Figs. 1a,d show the microstructures of the as cast sample with lower C-Si content, which consists of autensite dendrites together with M_7C_3 eutectic carbides. It is seen that the austenite dendrites are discontinuous in the matrix and the eutectic carbides have a rod and plate shape which is typical for a hypoeutectic white cast iron. As shown in Fig. 1d, martensite is formed at the interface of carbides and austensite as well as in areas between the different eutectic carbides.

After annealing, the eutectic carbides revealed a small change in microstucture, as seen in Fig. 1b,e. The dendrites of austenite is replaced by (Fig. 1b) with plenty of secondary carbides in the matrix, and some martensite has formed at the interface of eutectic carbides (Fig. 1e). Formation of the secondary carbides, which ranged from 100 *nm* to 2 μm in size, is associated with bainite formation in the matrix. After the destablization treatment with a holding time of 1.5 hour at 930 °C, the secondary carbides precipitate in the matrix. This results in a reduction in the concentration of the alloying elements in the matrix, especially for carbon. Applying the subcritical heat treatment (650 °C-2 h), austenite is transformed to bainite with secondary carbides and the remaining austensite has transformed directly to martensite after quenching the sample from 600 °C.

Similarly, after hardening the sample, the eutectic carbides are slightly affected as seen in Fig. 1c,f. The matrix has transformed mainly to martensite with secondary carbides. It was observed that the secondary carbides exhibited a finer size relative to the annealed sample. As the sample was taken through the destabilization cycle at 930 °C for 1.5 h, formation of the secondary carbides has reduced the carbon content in the matrix, and therefore the M_s temperature has increased. After quenching the sample from 930 °C, the austenite matrix is transformed to martensite. Since there is limited time for the secondary carbides to grow further, their average size is smaller than that for the annealed sample.

3.2. Microstructural analysis of samples with higher C-Si contents

Materials with higher C-Si contents were also studied in the as cast, annealed, and hardened conditions. In these samples, silicon contents were increased from 0.8 *wt*.% to 1.47 *wt*.% and carbon contents from 2.71 *wt*.% to 2.95 *wt*.%. The higher carbon content increases the volume fraction of the carbides' and the higher silicon increases carbon activity and decreases the stability of austenite(Kosasu, et al., 2012). During solidification, plenty of coarse primary carbides are developed in the form of long needles which are later surrounded by the eutectic carbides. The volume fraction of the primary and eutectic carbides are larger in this case than in the as cast sample with lower C-Si, and the carbides' distribution increased the inhomogenity and orientation in the microstructure. Further, a small volume of secondary carbides are observed in the bainitic matrix. After the

annealing heat treatment, the matrix is transformed to pearlite with secondary carbides. In the hardened sample, the matrix consists of martensite and secondary carbides. However, no changes in the primary carbides and eutectic carbides were observed (Fig. 2).

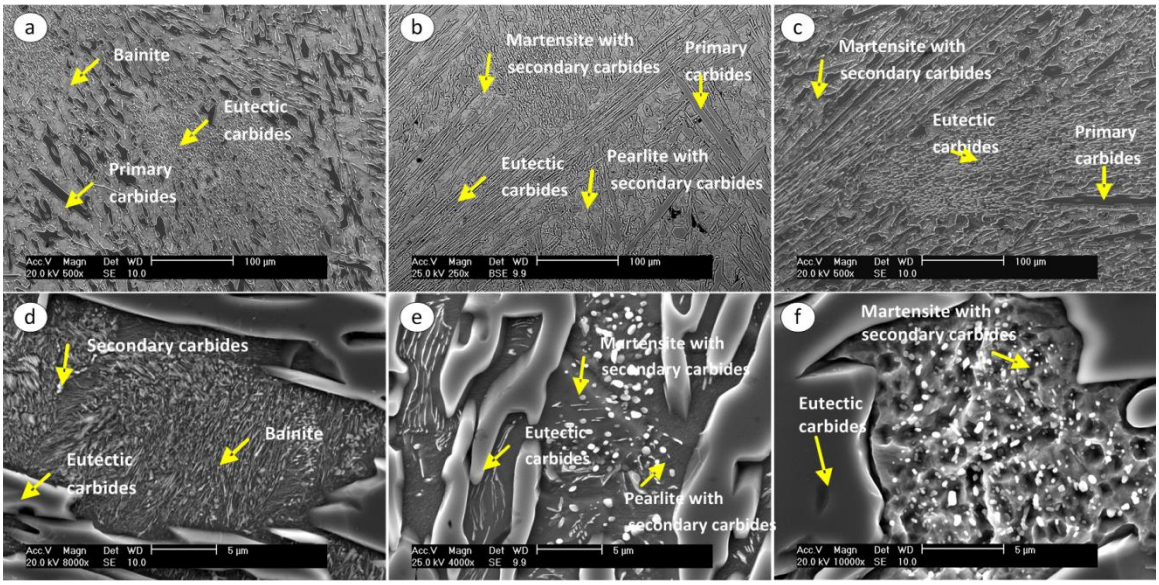

Fig. 2. Microstructures of high chromium white cast irons (higher C-Si contents) in the as cast (a, d), annealed (b,e) and hardened condition (c, f).

Figs. 2a,d show the microstructure of the as cast sample (higher C-Si content) where the dendrites of austenite appear to have disappeared into the matrix and the coarse primary carbides are widely distributed in the microstructure. In Fig. 2d, the matrix is made of bainite formed during cooling, similar to the annealed sample with lower C-Si contents. In addition, there are some secondary carbides in the matrix. Annealing does not affect the primary and eutectic carbides in the microstructure (Figs. 2b,e) and the matrix formed is pearlite with some martensite and plenty of secondary carbides which exhibit either cubic mophology or a fiber-like shape. These results are comparable to those for lower C-Si samples, except for the pearlite matrix.

In the hardened sample (Figs. 2c,f), while the eutectic carbides are not affected, the matrix has transformed to martensite. Fig. 4f shows the presence of fine secondary carbide, virtually all the particles are of submicron size. The composition of the of the secondary carbides is mainly M_7C_3, with some corresponding to $M_{23}C_6$. The matrix transformation is similar to that in the hardened sample with lower C-Si contents.

4. GRID INDENTATION AND RESULTS

The mechanical properties of various phases present in the materials and their volume fractions were determined by the grid indentation approach which is based on a large array of nanoindentation tests performed at random locations on the surface of the chosen multiphase material (Constantinides, et al., 2006). This technique is often used for mapping the mechanical properties over a certain area on the surface of the material. It has the potential to extract the mechanical properties of the indented phase provided the indentation depth is carefully chosen to minimize the influence of the surrounding medium. The mechanical properties of the various phases such as young's modulus and hardness as well as their volume fractions was determined from the tests using statistical methods (Randall, et al., 2009). As the surface roughness increases, results show large deviations from the mean value and this introduces a limitation on the number of indentations that can be made per unit area (Qasmi and Delobelle, 2006). Experimental results from a large number of indentations performed at random locations on the surface of a multiphase material can be presented as histograms or frequency plots of the measured properties (indentation hardness, H; indentation modulus, E_{IT}, etc.). Multiple peaks in the plot correspond to the various phases in the material (Němeček, et al., 2013). The test results were analyzed by a Weibull mixture model and the mean values and the standard deviations of the mechanical properties of the phases were determined. The nanoindentation performed in this investigation has penetration depths less than 225 nm, and each marker is smaller than the grain size of each phase (Fig. 3a). The load-depth curves (Fig. 3b) show three groups clearly in Fig. 3b. After fitting the data assuming Weibull mixture model, the CDF curves of Nanohardness have been redrawn with a deviation of 1.05 % as shown in Figs. 3c,d.

Fig. 3 demonstrates a typical grid indentation data and analysis set, in which the optical micrograph represents the area of material covered by grid indentation in the as cast sample with lower C-Si content. Hardness and other mechanical properties were extracted from loading and unloading curves, and then the hardness distribution and related volume fraction were analysed statistically (Ståhl, 2012).

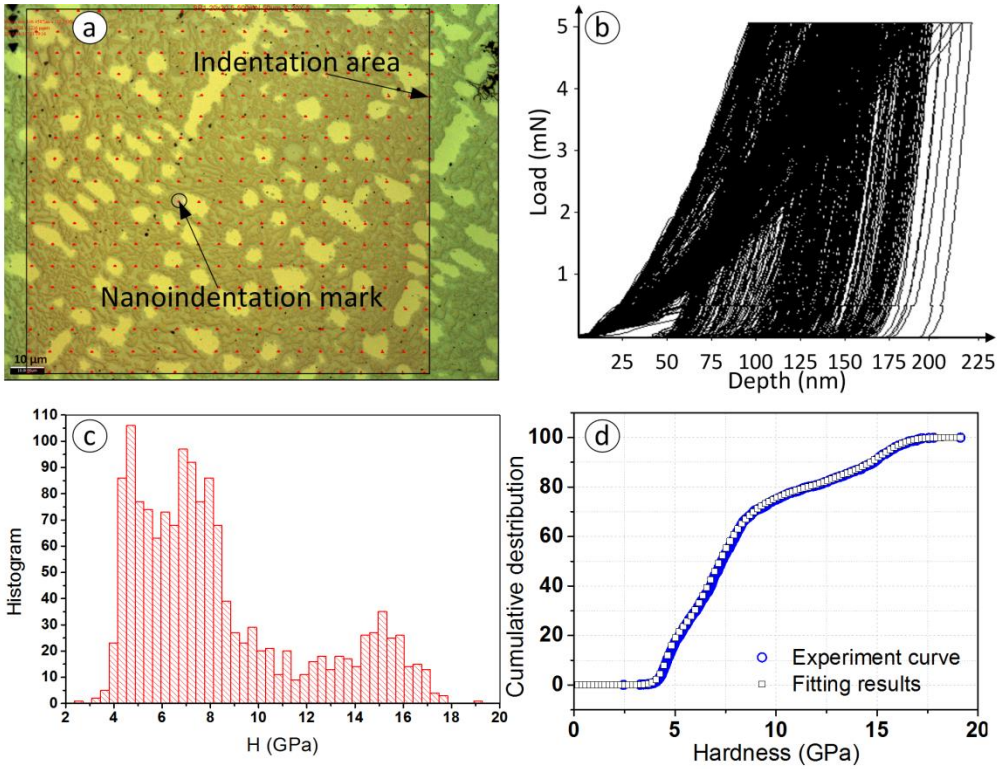

Fig. 3. Grid indentation data and analysis. (a) microstructure of the indentation marker under the optical microscope; (b) loading and unloading curves of indentation; (c) histogram from test data; (d) Curve fitted according to Weibull distribution.

The results of the grid indentation test on the as cast, annealed and hardened materials with lower C-Si content are shown in Figs. 4a-c in the form of hardness histograms. These histograms were obtained using the Weibull mixture model through which the indentation responses on different phases in the materials were extracted. In the cast sample, three distinct peaks are visible in Fig. 4a: one peak corresponding to austentic phase (23.7 vol.%) with a mean hardness of 4.73 GPa; a second peak corresponding to martensite phase (51.2 vol.%) with a hardness of 6.88 GPa; and the third peak corresponding to eutectic carbides (14.89 vol.%) with a hardness of 15.38 GPa. Although peaks from austenite and martensite were overlapping, the fitting method was robust enough to distinguish the two. These results are also confirmed by the results from microscopy. The small peak (12.5 GPa and 10.12% of volume fraction) observed between the second and third peaks could correspond to an overlap between eutectic carbides and martensite.

Grid indentation results for the annealed and hardened samples are shown in Figs. 4b,c in the form of hardness histograms. As mentioned before, Weibull mixture model was employed to fit the hardness values.For the annealed sample, the first peak corresponds to the bainite phase (58.5 vol.%) with a hardness of 4.197 GPa. A relatively smaller amout of martensite (20.6 vol.%) was responsible for the second peak with a hardness of 6 – 7 GPa. The third peak corresponds to the eutectic carbide (20.9 vol.%) and corresponds to 16.4 GPa. In the hardened sample, two major peaks and a minor one between them were found in the histogram. Martensite clearly plays a dominant role in this material, which is associated with the first peak in the hardness histogram. Eutectic carbides (22.3 vol.%) contributed to the second peak with hardness of 15.35 GPa. The response from the mixture of martensite and secondary carbides (8.9 vol.%) may be associated with the small peak with an average hardness of 10.12 GPa.

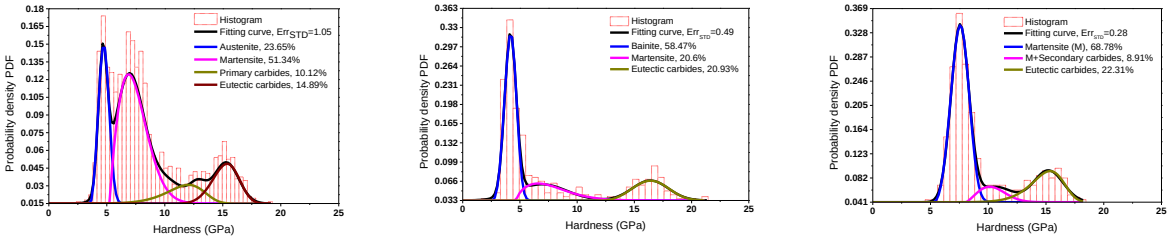

(a) As cast (b) Annealed (c) Hardened

Fig. 4. Hardness distribution and phase analysis from grid nanoindentation test on lower C-Si content materials.

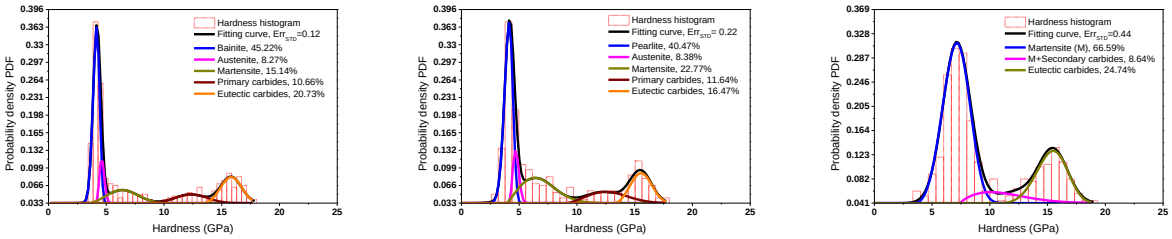

(a) As cast (b) Annealed (c) Hardened

Fig. 5. Hardness distribution and phase analysis from grid nanoindentation test on higher C-Si content materials.

Hardness data for samples containing C-Si contents are shown in Fig. 5. The three samples have a similar hardness distribution for eutectic carbides, but the matrix is different with distinct peaks. In the as cast sample, five peaks were found in the hardness histogram. Based on the hardness values for the invidual phases, five phases can be identified. The first peak may correspond to bainite (45.2 vol.%); the second peak is probably associated with austenite (8.3 vol.%); the third peak relates to martensite (15.1 vol.%); the fourth and fifth peaks correspond to primary carbide (10.7 vol.%) and eutectic carbide (20.7 vol.%) respectively. After annealing, the hardness distribution shows one peak for the matrix Hardness: 4.12 GPa), which is softer than in the as cast sample. After the hardening treatment, the matrix is transformed totally to martensite (Hardness: 7.14 GPa).

Fig. 6 shows a comparison of the hardness data for samples with lower and higher C-Si contents. For the sample with higher C-Si, there are two peaks for the carbides at 12.38 GPa for the primary carbides and at 15.57 GPa for eutectic carbides. Both the carbides have a similar phase content (17.8 vol.%). The matrix consists of only bainite (57.7 vol.%), and has a hardness of 4.16 GPa. After annealing, the matrix remains almost the same, but the eutectic carbides grow to larger sizes, and the hardness decreases. Since there are plenty of plate-like carbides around the eutectic carbides and primary carbides, there is no longer a clear peak for the carbides. The carbides are softened by the annealing treatment. After hardening, the matrix is transformed to martensite (69.8 vol.%), with a hardness of 6.8 GPa. Only the primary carbides (14.01 GPa) remain as the eutectic carbides are not stable during the heat treatment.

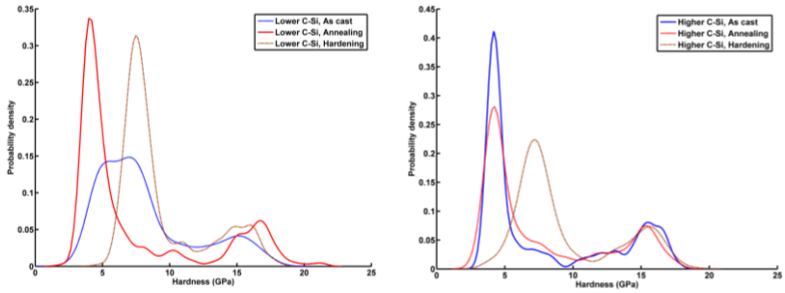

(a) (b)

Fig. 6. The effect of the heat treatment on (a) lower C-Si and (b) higher C-Si material.

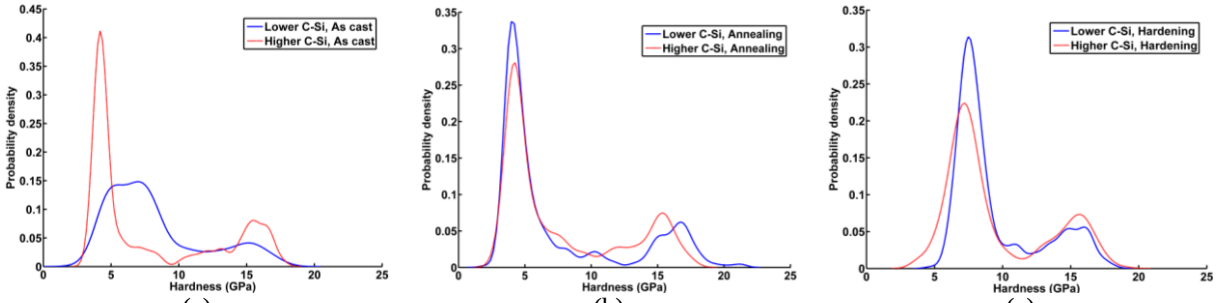

(a) (b) (c)

Fig. 7. The effect of the composition in three different heat treatment (a) as cast (b) annealed (c) hardened.

Fig. 7a shows a comparison of the as-cast materials and it is seen that the lower C-Si material is harder relative to the higher C-Si alloy. After annealing (Fig. 7b), a similar hardness is observed in the matrix corresponding to both compositions, although a larger amount of carbides are seen in the lower C-Si material. The hardening treatment transforms the matrix to martensite, leaving the carbides almost at the same level and the curves for both compositions are similar (Fig. 7c). With reference to the peaks associated with the individual phases, heat treatment does not seem to have any effect on the distribution of bainite and the eutectic carbides.

5. CONCLUSIONS

The effect of heat treatment on white cast irons with C-Si contents has been studied using nanoindentation technique, scanning electron microscopy and energy dispersive spectroscopy. Micromechanical properties such as hardness and modulus and the distribution of carbide and matrix phases were characterized using grid nanoindentation. Results have shown that both material composition (*C-Si* contents) and heat treatment strongly influence the microstructure and mechanical properties of the materials. An as-cast sample with higher C-Si content has more eutectic carbides in the microstructure and a softer matrix consisting of bainite, while a sample with lower C-Si content has a harder matrix containing austenite and martensite. After annealing treatment, both sets of materials are softer than before; however, the material containing higher carbon and silicon contents contains more eutectic carbides and is a little harder than the lower *C-Si* contents while the matrix has similar hardness. A small difference in hardness is observed after the hardening treatment. In both cases, secondary carbides and martensite surrounding the interconnecting eutectic carbides have been observed. However, the larger volume fraction of the primary carbides in the material with higher carbon and silicon contents leads to a reduction in the hardening effect.

ACKOWNLEDGMENT

This research is a part of the strategic research program the Sustainable Production Initiative SPI, cooperation between Lund University and Chalmers University of Technology. Author would like to thank Xylem Water Solution AB for providing the work materials and support. One of the authors (L. C.) appreciates the financial support by Chinese Scholarship Council.

REFERENCES

Asensio, J., J. A. Pero-Sanz and J. I. Verdeja (2003). "Microstructure selection criteria for cast irons with more than 10 wt.% chromium for wear applications." *Materials Characterization* **49**(2): 83-93.

B. Hinckley, K. F. D., R. Wuhrer, W. Yeung and A. Ray (2008). "SEM investigation of heat treated high-chromium cast irons." *Material Forum* **32**: 17.

Constantinides, G., K. S. Ravi Chandran, F. J. Ulm and K. J. Van Vliet (2006). "Grid indentation analysis of composite microstructure and mechanics: Principles and validation." *Materials Science and Engineering: A* **430**(1-2): 189-202.

Fernandez-Pariente, I. and F. J. Belzunce (2008). "Wear and oxidation behaviour of high-chromium white cast irons." *Materials Characterization* **59**(6): 669-674.

Huang, Y., Y. K. Chou and S. Y. Liang (2006). "CBN tool wear in hard turning: a survey on research progresses." *The International Journal of Advanced Manufacturing Technology* **35**(5-6): 443-453.

Karantzalis, A. E., A. Lekatou and H. Mavros (2009). "Microstructural Modifications of As-Cast High-Chromium White Iron by Heat Treatment." *Journal of Materials Engineering and Performance* **18**(2): 174-181.

Němeček, J., V. Králík and J. Vondřejc (2013). "Micromechanical analysis of heterogeneous structural materials." *Cement and Concrete Composites* **36**: 85-92.

P. Kosasu, S. I., P. Srichareonchai, Y. Matsubara (2012). "Effect of Silicon on subcritical heat treatment behavior and wear resistance of 16 wt% Cr cast iron with 2 wt% Mo." *Journal of metals, materials and minerals* **22**(2): 89-95.

Qasmi, M. and P. Delobelle (2006). "Influence of the average roughness R-ms on the precision of the Young's modulus and hardness determination using nanoindentation technique with a Berkovich indenter." *Surface & Coatings Technology* **201**(3-4): 1191-1199.

Randall, N. X., M. Vandamme and F. J. Ulm (2009). "Nanoindentation analysis as a two-dimensional tool for mapping the mechanical properties of complex surfaces." *Journal of Materials Research* **24**(3): 679-690.

Ståhl, J. E. (2012), Metal Cutting – Theory and models, ISBN 978-91-637-1336-1, Lund/Fågersta.

Tabrett, Christopher P (1997), "Microstructure-property relationships in high chromium white irons. ", *thesis (Ph. D) , University of South Australia*: 5-26.

Tsypin, I. I. (1969). "Machinability of Wear-Resistant Chromium Cast-Irons." *Russian Engineering Journal-Ussr* **49**(11): 71-&.

Turenne, S., F. Lavallee and J. Masounave (1989). "Matrix Microstructure Effect on the Abrasion Wear-Resistance of High-Chromium White Cast-Iron." *Journal of Materials Science* **24**(8): 3021-3028.

Vander Voort, George F. (2004). ASM Handbook, Volume 09 - Metallography and Microstructures. *ASM International*: 565-587.